

# Fast Sampling for Linear Inverse Problems of Vectors and Tensors using Multilinear Extensions

Hao Li, Dong Liang, Zixi Zhou, Zheng Xie

**Abstract**—Sampling vector and tensor signals is the process of choosing sites in vectors and tensors to place sensors in order to effectively recover the whole signals from a limited number of observations by solving linear inverse problems (LIPs). Here, we present closed-form multilinear extensions for the frame potential of pruned matrices, and based on these, we develop an algorithm named fast Frank-Wolfe algorithm for sampling vectors and tensors with low complexity. Then we provide the approximation factor of our proposed algorithm for a special class of sampling matrices. Then, we conduct experiments to verify the higher performance and lower complexity of our proposed algorithm. Finally, we demonstrate that FFW sampling and least squares reconstruction yield superior results for image data compared to convCNP completion with random sampling.

**Index Terms**—Inverse problem, multilinear extension, sampling, tensors.

## I. INTRODUCTION

**R**EAL world discrete signals like audio, images and videos can be mathematically described as vectors, matrices, or higher-order tensors that reside in various modes [1], [2]. A target signal can be retrieved from incomplete samples by solving a linear inverse problem (LIP), which is generally considered to be linear in the remaining factor mode(s) with low-dimensional parameters [3]. It is crucial for applications where signal acquisition is expensive or time-consuming to intelligently select partial entries of a signal for better reconstruction through sampling for LIPs [4], such as sensor signals in wireless communication [5], labels on medical images [6], and ratings in recommendation systems [7]. Essentially a combinatorial problem, the sampling problem is very challenging to solve, even for small-scale issues. Therefore, generating a suboptimal sampling strategy with a quality guarantee is crucial. The commonly used quality guarantee is the approximation factor, which is the ratio of the value of the suboptimal solution to the value of the best solution.

Suppose that the samples are corrupted by independently and identically distributed (i.i.d.) noise, the quantity and quality of observed samples will have a significant impact on the reconstructed mean square error (MSE) of the unbiased least-squares (LS) solution [8]. As a result, extensive literature has examined sampling methods to reduce reconstruction MSE while working within a limited sampling budget.

Sampling vectors has been applied in sensor placement to deploy sensors for monitoring a physical field. The sensor

placement problem was initially described as a nonconvex optimization problem by [9], and was relaxed into a convex problem that can be solved using interior point methods with polynomial complexity. However, when the sensor budget was very small, this relaxation strategy worked badly. After that, greedy algorithms were created to choose sensor locations one by one by solving various local optimization problems to improve MSE performance [8], [10], [11]. [11] introduced FrameSense, which preserves the sub-modularity property and has theoretically bounded performance. The worst-case MSE function was used as the objective to select samples utilizing developed efficient algorithms in [8]. However, the computation of the eigenspace corresponding to the chosen sensors was necessary for each greedy search, and it is expensive when the eigenspace dimension is large. A fast MSE pursuit algorithm was recently proposed by [10] to greedily reduce an approximate MSE criterion. However, this algorithm was still plagued by repeated matrix inverse calculations.

Although there are numerous sampling methods for vector signals, the high cost of computation and storage prevents them from being used for higher-order tensor signals. Therefore, [12] developed a multi-domain frame potential-based sampling strategy to address these issues by designing samples in each order and then combining their intersection tensor as the chosen data. The proposed sampling methods utilized factor matrices directly since their sampling matrix has the Kronecker product structure. Additionally, [13], [14] described three structured sub-Nyquist sampling methods for tensor signal querying. These methods were referred to as slab sampling, fiber sampling, and entry sampling, respectively. These sample techniques cannot reach arbitrary sampling budgets, despite their minimal complexity. A fast MSE-based and unstructured sampling technique for linear-model signals ranging from vectors to tensors was recently proposed by [15]. This method works well for vector signals, but it has a high computational complexity for high-order tensors.

We make three contributions. First, we provide closed-form multilinear extensions for the frame potential of pruned matrices. Second, we propose a fast algorithm (FFW) for sampling vector signals, and its solution is guaranteed to be close to the optimal one in a special case. Third, we extend FFW to sampling tensor signals, and also give the guarantee of solution quality. We experimentally compare FFW with FrameSense [11], Greedy FP [12] and the recently proposed FMBS [15] to verify the effectiveness of our proposed algorithm.

Hao Li, Dong Liang, Zixi Zhou, Zheng Xie are with College of Science, National University of Defense Technology, Changsha, 410073, Hunan, China (e-mail:)

## II. PROBLEM STATEMENTS

Throughout this paper, we use  $(\cdot)^\dagger$  to represent Moore-Penrose pseudoinverse,  $(\cdot)^T$  and  $\langle \cdot, \cdot \rangle$  to represent transposition and the inner product, respectively. The exception operator is denoted by  $\mathbb{E}\{\cdot\}$ .  $\otimes$  represents the Kronecker product, and some important properties of Kronecker product can be seen in [16].

A tensor  $\mathcal{X} \in \mathbb{R}^{N_1 \times \dots \times N_R}$  of order  $R$  can be viewed as a discretized multidomain signal, with each of its entries indexed over  $R$  different domains. Two tensors  $\mathcal{X} \in \mathbb{R}^{N_1 \times \dots \times N_R}$  and  $\mathcal{G} \in \mathbb{R}^{K_1 \times \dots \times K_R}$  can be related by a multilinear system of equations as

$$\mathcal{X} = \mathcal{G} \bullet_1 \mathbf{U}_1 \bullet_2 \dots \bullet_R \mathbf{U}_R, \quad (1)$$

where  $\{\mathbf{U}_r \in \mathbb{R}^{N_r \times K_r}\}_{r=1}^R$  represents a set of factor matrices that relates each domain of  $\mathcal{X}$  and  $\mathcal{G}$ , and  $\bullet_r$  represents the  $r$ -th mode product between a tensor and a matrix [17]. Vectorizing (1), we have

$$\mathbf{x} = (\mathbf{U}_1 \otimes \dots \otimes \mathbf{U}_R) \mathbf{g} \quad (2)$$

with  $\mathbf{x} = \text{vec}(\mathcal{X}) \in \mathbb{R}^{\tilde{N}}$ ,  $\tilde{N} = \prod_{r=1}^R N_r$ , and  $\mathbf{g} = \text{vec}(\mathcal{G}) \in \mathbb{R}^{\tilde{K}}$ ,  $\tilde{K} = \prod_{r=1}^R K_r$ .

In this paper, we are concerned with sampling a tensor  $\mathcal{X}$ , which is equivalent to selecting entries of  $\mathbf{x} = \text{vec}(\mathcal{X})$ . Suppose that the set of matrices  $\{\mathbf{U}_r\}_{r=1}^R$  are perfectly known, and that each of them is tall, i.e.,  $N_r > K_r$  for  $r = 1, \dots, R$ , and has full column rank.

Let  $\mathcal{N}_r$  be the set of all row indices of the matrix  $\mathbf{U}_r$  and  $\mathcal{L}_r$  be the set of selected row indices from  $\mathcal{N}_r$ ,  $r = 1, \dots, R$ . In order to circumvent the curse of dimensionality, Ortiz-Jimenez et al. [12] defined a sampling matrix

$$\Phi(\mathcal{L}) := \Phi_1(\mathcal{L}_1) \otimes \dots \otimes \Phi_R(\mathcal{L}_R),$$

where  $\mathcal{L} = \bigcup_{r=1}^R \mathcal{L}_r$  and  $\Phi_r(\mathcal{L}_r)$  is a selection matrix for  $\mathbf{U}_r$ ,  $r = 1, \dots, R$ . Then, sampling a tensor can be performed independently for each domain, that is

$$\begin{aligned} \mathbf{y} &= \Phi(\mathcal{L})\mathbf{x} \\ &= (\Phi_1(\mathcal{L}_1) \otimes \dots \otimes \Phi_R(\mathcal{L}_R)) (\mathbf{U}_1 \otimes \dots \otimes \mathbf{U}_R) \mathbf{g} \\ &= (\Phi_1(\mathcal{L}_1) \mathbf{U}_1 \otimes \dots \otimes \Phi_R(\mathcal{L}_R) \mathbf{U}_R) \mathbf{g}. \end{aligned} \quad (3)$$

Let  $|\mathcal{L}_r| = L_r$  be the number of selected sensors per domain and  $|\mathcal{L}| = \sum_{r=1}^R L_r = L$  be the total number of selected sensors.

Denote  $\Psi(\mathcal{L}) = \Phi_1(\mathcal{L}_1) \mathbf{U}_1 \otimes \dots \otimes \Phi_R(\mathcal{L}_R) \mathbf{U}_R$ . Notice that (3) is overdetermined, by least squares, we can estimate the core as

$$\hat{\mathbf{g}} = \Psi^\dagger(\mathcal{L})\mathbf{y} = \left[ (\Phi_1(\mathcal{L}_1) \mathbf{U}_1)^\dagger \otimes \dots \otimes (\Phi_R(\mathcal{L}_R) \mathbf{U}_R)^\dagger \right] \mathbf{y},$$

and then reconstruct  $\hat{\mathbf{x}}$  by (2).

Suppose the measurements collected in  $\mathbf{y}$  are perturbed by zero-mean white Gaussian noise with unit variance, then the least-squares solution has the inverse error covariance or the Fisher information matrix  $\mathbf{T}(\mathcal{L}) = \mathbb{E}\{(\mathbf{g} - \hat{\mathbf{g}})(\mathbf{g} - \hat{\mathbf{g}})^T\} = \Psi^T(\mathcal{L})\Psi(\mathcal{L})$  that determines the quality of the estimators  $\hat{\mathbf{g}}$ . Thus, a sampling problem can be posed as a discrete optimization problem that finds the best sampling subset by optimizing a scalar function of  $\mathbf{T}(\mathcal{L})$ . The most popular scalar function is

the mean squared error  $\text{MSE}(\Psi(\mathcal{L})) = \text{tr}\{\mathbf{T}^{-1}(\mathcal{L})\}$ , which is difficult to minimize as it is neither convex, nor submodular.

The frame potential (FP) [18] of the matrix  $\Psi(\mathcal{L})$  is defined as  $\text{FP}(\Psi(\mathcal{L})) := \text{tr}\{\mathbf{T}^T(\mathcal{L})\mathbf{T}(\mathcal{L})\}$ . According to [11], FP can be related to the MSE as

$$c_1 \frac{\text{FP}(\Psi(\mathcal{L}))}{\lambda_{\max}^2\{\mathbf{T}(\mathcal{L})\}} \leq \text{MSE}(\Psi(\mathcal{L})) \leq c_2 \frac{\text{FP}(\Psi(\mathcal{L}))}{\lambda_{\min}^2\{\mathbf{T}(\mathcal{L})\}},$$

where  $c_1$ , and  $c_2$  are constants that depend on the data model. From the above bound, it is clear that one can minimize  $\text{MSE}(\Psi(\mathcal{L}))$  by minimizing  $\text{FP}(\Psi(\mathcal{L}))$ .

By [12], the frame potential of  $\Psi(\mathcal{L})$  can be expressed as

$$\text{FP}(\Psi(\mathcal{L})) = \prod_{r=1}^R \text{FP}(\Psi_r(\mathcal{L}_r)) = \prod_{r=1}^R \text{tr}\{\mathbf{T}_r^T(\mathcal{L}_r)\mathbf{T}_r(\mathcal{L}_r)\} \quad (4)$$

where  $\mathbf{T}_r(\mathcal{L}_r) = \Psi_r^T(\mathcal{L}_r)\Psi_r(\mathcal{L}_r)$ ,  $\Psi_r(\mathcal{L}_r) = \Phi_r(\mathcal{L}_r)\mathbf{U}_r$ .

For brevity, let

$$F(\mathcal{S}) := \text{FP}(\Psi(\mathcal{N} \setminus \mathcal{S})) = \prod_{r=1}^R F_r(\mathcal{S}_r) := \prod_{r=1}^R \text{FP}(\Psi_r(\mathcal{N}_r \setminus \mathcal{S}_r)),$$

where  $\mathcal{S} = \bigcup_{i=1}^R \mathcal{S}_i$  and  $\mathcal{S}_i \cap \mathcal{S}_j = \emptyset$  for  $i \neq j$ .

Denote  $N = \sum_{r=1}^R N_r$  and  $K = \sum_{r=1}^R K_r$ . Then we state the sampling problem as

$$\begin{aligned} \min_{\mathcal{S}_1, \dots, \mathcal{S}_R} F(\mathcal{S}) &= \prod_{r=1}^R \text{FP}(\Psi_r(\mathcal{N}_r \setminus \mathcal{S}_r)) \\ \text{s.t.} \quad \sum_{r=1}^R |\mathcal{S}_r| &= N - L. \end{aligned} \quad (5)$$

Sampling vectors and tensors is Problem (5) with  $R = 1$  and  $R \geq 2$ , respectively.

In the rest of this paper,  $\Psi_r(\mathcal{N}_r)$  will be represented as  $\Psi_r$  and  $\Psi = \Psi_1 \otimes \dots \otimes \Psi_R$  whenever such substitution does not introduce ambiguity.

## III. PRELIMINARIES

In this section, in order to overcome the defect that the discrete function cannot be derived, we give the multilinear relaxation of  $F(\mathcal{S})$  to transform  $F(\mathcal{S})$  into a continuous function. The set function  $F(\mathcal{S})$  is defined on the vertices of the hypercube  $\{0, 1\}^N$  and each vertex is the indicator vector of a set. The multilinear extension  $\tilde{F}$  of  $F(\mathcal{S})$  is defined as

$$\tilde{F}(\mathbf{x}) := \mathbb{E}_{\mathcal{S} \sim \mathbf{x}} [F(\mathcal{S})] = \sum_{\mathcal{S} \subseteq \mathcal{N}} F(\mathcal{S}) \prod_{j \in \mathcal{S}} x_j \prod_{j \notin \mathcal{S}} (1 - x_j),$$

where  $\mathcal{S} \sim \mathbf{x}$  denotes that  $\mathcal{S}$  is drawn from the independent distribution with marginals  $x \in [0, 1]^N$ . One can see that for any set  $\mathcal{S}$  and its indicator vector  $\mathbf{1}_{\mathcal{S}}$ ,  $\tilde{F}(\mathbf{1}_{\mathcal{S}}) = F(\mathcal{S})$ . The following theorem shows the closed-form of  $\tilde{F}(\mathbf{x})$ .

*Theorem 1:* Let  $p_{ab}^r$  be the  $(a, b)$ -element of  $\Psi_r$ . The multilinear extension of  $F(\mathcal{S})$  can be expressed as

$$\tilde{F}(\mathbf{x}) = \prod_{r=1}^R \tilde{F}_r(\mathbf{x}^r) = \prod_{r=1}^R \left\{ \sum_{i=1}^{K_r} \sum_{j=1}^{K_r} \left[ \sum_{n=1}^{N_r} (1 - x_n^r) p_{ni}^r p_{nj}^r \right]^2 \right\},$$

where  $\mathbf{x} = (\mathbf{x}^1, \mathbf{x}^2, \dots, \mathbf{x}^R)$  and  $\mathbf{x}^r = (x_1^r, x_2^r, \dots, x_{N_r}^r)$ ,  $r = 1, \dots, R$ .

*Proof:* Note that  $\tilde{F}(\mathbf{x})$  is the expected value of  $F(\mathcal{S})$  over the independent distribution with marginals  $\mathbf{x}$ , we have

$$\tilde{F}(\mathbf{x}) = \mathbb{E}_{\mathcal{S} \sim \mathbf{x}} [F(\mathcal{S})] = \prod_{r=1}^R \tilde{F}_r(\mathbf{x}^r) := \prod_{r=1}^R \mathbb{E}_{\mathcal{S}_r \sim \mathbf{x}^r} [F_r(\mathcal{S}_r)].$$

By the definitions of  $\tilde{F}_r(\mathbf{x}^r)$  and  $F(\mathcal{S})$ , we obtain

$$\begin{aligned} \tilde{F}_r(\mathbf{x}^r) &= \sum_{\mathcal{S}_r \subseteq \mathcal{N}_r} F_r(\mathcal{S}_r) \prod_{j \in \mathcal{S}_r} x_j^r \prod_{j \in \mathcal{N}_r \setminus \mathcal{S}_r} (1 - x_j^r) \\ &= \sum_{\mathcal{S}_r \subseteq \mathcal{N}_r} \text{FP}(\Psi_r(\mathcal{N}_r \setminus \mathcal{S}_r)) \prod_{j \in \mathcal{S}_r} x_j^r \prod_{j \in \mathcal{N}_r \setminus \mathcal{S}_r} (1 - x_j^r) \\ &= \sum_{\mathcal{S}_r \subseteq \mathcal{N}_r} \text{FP}(\Psi_r(\mathcal{S}_r)) \prod_{j \in \mathcal{S}_r} (1 - x_j^r) \prod_{j \in \mathcal{N}_r \setminus \mathcal{S}_r} x_j^r \\ &= \sum_{\mathcal{S}_r \subseteq \mathcal{N}_r} \text{tr} \{ \mathbf{T}_r^T(\mathcal{S}_r)^* \mathbf{T}_r(\mathcal{S}_r) \} \prod_{j \in \mathcal{S}_r} (1 - x_j^r) \prod_{j \in \mathcal{N}_r \setminus \mathcal{S}_r} x_j^r \\ &= \sum_{\mathcal{S}_r \subseteq \mathcal{N}_r} \sum_{a=1}^{K_r} \sum_{b=1}^{K_r} [\mathbf{T}_r(\mathcal{S}_r)_{ab}]^2 \prod_{j \in \mathcal{S}_r} (1 - x_j^r) \prod_{j \in \mathcal{N}_r \setminus \mathcal{S}_r} x_j^r \\ &= \sum_{a=1}^{K_r} \sum_{b=1}^{K_r} \sum_{\mathcal{S}_r \subseteq \mathcal{N}_r} [\mathbf{T}_r(\mathcal{S}_r)_{ab}]^2 \prod_{j \in \mathcal{S}_r} (1 - x_j^r) \prod_{j \in \mathcal{N}_r \setminus \mathcal{S}_r} x_j^r \\ &= \sum_{a=1}^{K_r} \sum_{b=1}^{K_r} \mathbb{E}_{\mathcal{S}_r \sim (1_{N_r} - \mathbf{x}^r)} [\mathbf{T}_r(\mathcal{S}_r)_{ab}]^2, \end{aligned}$$

where  $\mathbf{T}_r(\mathcal{S}_r)_{ab}$  denotes the  $(a, b)$ -element of  $\mathbf{T}_r(\mathcal{S}_r)$ . Then, we have

$$\begin{aligned} \mathbb{E}_{\mathcal{S}_r \sim (1_{N_r} - \mathbf{x}^r)} [\mathbf{T}_r(\mathcal{S}_r)_{ab}]^2 &= \left\{ \mathbb{E}_{\mathcal{S}_r \sim (1_{N_r} - \mathbf{x}^r)} [\mathbf{T}_r(\mathcal{S}_r)_{ab}] \right\}^2 \\ &= \left\{ \mathbb{E}_{\mathcal{S}_r \sim (1_{N_r} - \mathbf{x}^r)} \left[ \sum_{n \in \mathcal{S}_r} p_{na}^r p_{nb}^r \right] \right\}^2 \\ &= \left[ \sum_{n=1}^{N_r} (1 - x_n^r) p_{na}^r p_{nb}^r \right]^2. \end{aligned}$$

Therefore, we conclude that

$$\tilde{F}_r(\mathbf{x}^r) = \sum_{i=1}^{K_r} \sum_{j=1}^{K_r} \left[ \sum_{n=1}^{N_r} (1 - x_n^r) p_{ni}^r p_{nj}^r \right]^2.$$

This completes the proof of Theorem 1.  $\blacksquare$

The general technique for minimizing  $\tilde{F}(\mathbf{x})$  is the continuous greedy algorithm [19], which is a slight modification of the Frank-Wolfe algorithm (FW) [20], with a fixed step size  $\delta = 1/N^2$ . In each iteration, the algorithm takes a step  $\mathbf{x}^{(t+1)} = \mathbf{x}^{(t)} + \delta \mathbf{h}^{(t)}$  in the direction

$$\mathbf{h}^{(t)} = \arg \min_{\mathbf{h}' \in \mathcal{P}} \langle \mathbf{h}', \nabla \tilde{F}(\mathbf{x}^{(t)}) \rangle,$$

where  $\mathcal{P}$  denotes the polytope corresponding to the family of feasible sets. However, for any step size  $\delta = 1/t$  with  $t \geq 2$ , this algorithm terminates in  $\mathcal{O}(t)$  iterations and gives a fractional solution. In order to round the fractional solution to an integral solution, the pipage rounding technique [19] is

needed, which requires  $\mathcal{O}(N^2)$  function calls. Obviously, this algorithm with  $t \geq 2$  is poorly suited for large-scale problems because of the excessive complexity of pipage rounding. Here, motivated by the continuous greedy algorithm, we design a fast algorithm with low complexity.

#### IV. ALGORITHM TO SAMPLING VECTORS

In this section, we focus on vector signals ( $R = 1$ ) and propose the Fast Frank-Wolfe algorithm (FFW) for computing suboptimal solution of Problem (5).

For vector signals where there is only one factor matrix, we have  $\Psi = \Psi_1$ ,  $N = N_1$ , and  $K = K_1$ . For convenience, denote  $\mathbf{x} = (x_1, x_2, \dots, x_N)$ ,  $p_{ab}$  the  $(a, b)$ -element of  $\Psi$  and  $P_i$  the  $i$ -th column of  $\Psi$ . The multilinear extension of  $F(\mathcal{S})$  can be expressed as

$$\tilde{F}(\mathbf{x}) = \sum_{i=1}^K \sum_{j=1}^K \left[ \sum_{n=1}^N (1 - x_n) p_{ni} p_{nj} \right]^2.$$

##### A. The Algorithm

---

**Algorithm 1** Fast Frank-Wolfe Algorithm for Vector Signals.

---

**Input:**  $\Psi = (p_{ab}) \in \mathbb{R}^{N \times K}$ ;  $L$

- 1: Compute  $m_{ij} = P_i^T P_j$ ,  $i = 1, \dots, K$ ,  $j = 1, \dots, K$
  - 2: Compute  $d_n = \sum_{i=1}^K \sum_{j=1}^K m_{ij} p_{ni} p_{nj}$ ,  $n = 1, \dots, N$
  - 3: Select the  $N - L$  elements with the biggest values from  $\{d_1, d_2, \dots, d_N\}$ , denoted as  $\{d_{l_1}, d_{l_2}, \dots, d_{l_{N-L}}\}$
  - 4: **Return:**  $\mathcal{S} = \{l_1, l_2, \dots, l_{N-L}\}$
- 

The computational complexity of step 1 and 2 is  $\mathcal{O}(NK^2)$  and the computational complexity of step 3 is  $\mathcal{O}(N)$ . Therefore, the total computational complexity of Algorithm 1 is  $\mathcal{O}(NK^2)$ . We compare the computational complexity with the following sampling methods for vector signals: FrameSense [11], minimum nonzero eigenvalue pursuit (MNEP) [8], maximal projection on minimum eigenspace (MPME) [8], fast MSE pursuit-based sampling (fastMSE) [10], and Fast MSE-Based Sampling (FMBS) [15]. The computational complexities of those methods and the proposed FFW are illustrated in Table I. One can see that FFW has the lowest complexity compared with other methods. Moreover, the complexity of FFW does not depend on  $L$ , therefore, the advantage of FFW is more prominent when  $K \ll L$ . In these methods, only FrameSense and FFW have theoretically bounded performance.

TABLE I  
COMPARISON OF COMPUTATIONAL COMPLEXITY OF DIFFERENT SAMPLING METHODS

Method	FrameSense [11]	MNEP [8]	MPME [8]
Complexity	$\mathcal{O}(N^3)$	$\mathcal{O}(NLK^3)$	$\mathcal{O}(NLK^2)$
Method	fastMSE [10]	FMBS [15]	FFW
Complexity	$\mathcal{O}(NLK^2)$	$\mathcal{O}(NL^2)$	$\mathcal{O}(NK^2)$

### B. Near-optimality of FFW for Vector Signals

Here, we give the approximation factor of Algorithm 1.

*Theorem 2:* Denote by  $\mathcal{S}^*$  an optimal solution of (5). If  $P_i^T P_j > 0$  and  $p_{ni}p_{nj} \geq 0$ ,  $n = 1, \dots, N$  for any  $i, j = 1, \dots, K$ , Algorithm 1 return a set  $\mathcal{S}$  such that  $G(\mathbf{1}_{\mathcal{S}}) > \frac{N}{N+L}G(\mathbf{1}_{\mathcal{S}^*})$ , where  $G(\mathbf{x}) = \tilde{F}(\mathbf{0}) - \tilde{F}(\mathbf{x})$ .

*Proof:* Let  $\mathcal{H} = \{\mathbf{x} \in \{0, 1\}^N \mid \|\mathbf{x}\|_1 = N - L\}$ . Note that  $G(\mathbf{0}) = 0$  and  $G(\mathbf{x})$  is a quadratic function,  $G(\mathbf{x})$  can be express as

$$G(\mathbf{x}) = D^T \mathbf{x} + \frac{1}{2} \mathbf{x}^T H \mathbf{x}, \quad (6)$$

where  $D = (d_1, d_2, \dots, d_N)$ ,

$$d_t = \left. \frac{\partial G(\mathbf{x})}{\partial x_t} \right|_{\mathbf{x}=\mathbf{0}} = 2 \sum_{i=1}^K \sum_{j=1}^K (P_i^T P_j \cdot p_{ti} p_{tj}) \quad (7)$$

and  $H = \{h_{s,t}\}_{N \times N}$ ,

$$h_{s,t} = \left. \frac{\partial^2 G(\mathbf{x})}{\partial x_t \partial x_s} \right|_{\mathbf{x}=\mathbf{0}} = -2 \sum_{i=1}^K \sum_{j=1}^K (p_{si} p_{sj} \cdot p_{ti} p_{tj}). \quad (8)$$

One can see that  $\mathbf{1}_{\mathcal{S}} \in \arg \max_{\mathbf{x} \in \mathcal{H}} D^T \mathbf{x}$  as  $\mathcal{S}$  is obtained by Algorithm 1. Substituting (7) and (8) in (6), we obtain

$$\begin{aligned} G(\mathbf{x}) &= 2 \sum_{i=1}^K \sum_{j=1}^K \left( P_i^T P_j \cdot \sum_{n=1}^N x_n p_{ni} p_{nj} \right) \\ &\quad - \sum_{i=1}^K \sum_{j=1}^K \left[ \sum_{n_1=1}^N \sum_{n_2=1}^N (x_{n_1} p_{n_1 i} p_{n_1 j} \cdot x_{n_2} p_{n_2 i} p_{n_2 j}) \right] \\ &= \sum_{i=1}^K \sum_{j=1}^K \left[ 2 P_i^T P_j \sum_{n=1}^N x_n p_{ni} p_{nj} - \left( \sum_{n=1}^N x_n p_{ni} p_{nj} \right)^2 \right]. \end{aligned}$$

Let  $\alpha_{ij} = P_i^T P_j$  and  $y_{ij} = \sum_{n=1}^N x_n p_{ni} p_{nj}$ ,  $i, j = 1, \dots, K$ . Note that  $\mathbf{x} \in \{0, 1\}^N$  and  $p_{ni} p_{nj} \geq 0$  for  $n = 1, \dots, N$ , we have  $\alpha_{ij} \geq y_{ij} \geq 0$ . Let  $M = \max_{\mathbf{x} \in \mathcal{H}} D^T \mathbf{x}$  and  $T(\mathbf{y}) = \sum_{i=1}^K \sum_{j=1}^K (y_{ij} - \alpha_{ij})^2$ ,  $\mathbf{y} = (y_{11}, \dots, y_{1K}, \dots, y_{K1}, \dots, y_{KK})^T$ , and we have

$$G(\mathbf{x}) = \sum_{i=1}^K \sum_{j=1}^K [2\alpha_{ij} \cdot y_{ij} - y_{ij}^2] = -T(\mathbf{y}) + \sum_{i=1}^K \sum_{j=1}^K \alpha_{ij}^2.$$

Suppose that the  $y_{ij}$ ,  $i, j = 1, \dots, K$  are independent variables, and denote by  $T_{\min}(T_{\max})$  the value of

$$\begin{aligned} &\min_{\mathbf{y}} (\max) T(\mathbf{y}) \\ \text{s.t.} \quad &2 \sum_{i=1}^K \sum_{j=1}^K (\alpha_{ij} \cdot y_{ij}) = M \\ &\alpha_{ij} \geq y_{ij} \geq 0, \quad i, j = 1, \dots, K \end{aligned}$$

One can verify that

$$\begin{aligned} T_{\min} &= \sum_{i=1}^K \sum_{j=1}^K \left( \frac{M \alpha_{ij}}{2 \sum_{a=1}^K \sum_{b=1}^K \alpha_{ab}^2} - \alpha_{ij} \right)^2 \\ &= \left( \frac{M}{2 \sum_{a=1}^K \sum_{b=1}^K \alpha_{ab}^2} - 1 \right)^2 \sum_{i=1}^K \sum_{j=1}^K \alpha_{ij}^2. \end{aligned}$$

Moreover,  $T_{\min}$  is also the value of

$$\begin{aligned} &\min_{\mathbf{y}} T(\mathbf{y}) \\ \text{s.t.} \quad &2 \sum_{i=1}^K \sum_{j=1}^K (\alpha_{ij} \cdot y_{ij}) \leq M \\ &\alpha_{ij} \geq y_{ij} \geq 0, \quad i, j = 1, \dots, K \end{aligned}$$

In fact,  $y_{ij}$ ,  $i, j = 1, \dots, K$  are not independent, and are determined by  $\mathbf{x}$ , thus

$$\begin{aligned} G(\mathbf{1}_{\mathcal{S}^*}) &= \max_{\mathbf{x} \in \mathcal{H}} G(\mathbf{x}) \\ &< -T_{\min} + \sum_{i=1}^K \sum_{j=1}^K \alpha_{ij}^2 \\ &= \left\{ -\frac{1}{4} \left( \frac{M}{\sum_{i=1}^K \sum_{j=1}^K \alpha_{ij}^2} \right)^2 \right. \\ &\quad \left. + \left( \frac{M}{\sum_{i=1}^K \sum_{j=1}^K \alpha_{ij}^2} \right) \right\} \sum_{i=1}^K \sum_{j=1}^K \alpha_{ij}^2 \\ &= -\frac{1}{4} \frac{M^2}{\sum_{i=1}^K \sum_{j=1}^K \alpha_{ij}^2} + M. \end{aligned}$$

Now we consider  $G(\mathbf{1}_{\mathcal{S}})$ . Sort  $\alpha_{ij}$ ,  $i, j = 1, 2, \dots, K$  and renumber  $\alpha_{ij}$  by  $\alpha_1 \geq \alpha_2 \geq \dots \geq \alpha_{K^2}$ . There exist integer  $k$  and real number  $\delta$  such that  $\sum_{i=k}^{K^2} \alpha_i^2 \leq \frac{M}{2} < \sum_{i=k-1}^{K^2} \alpha_i^2$  and  $\sum_{i=k}^{K^2} \alpha_i^2 + \alpha_{k-1} \delta = \frac{M}{2}$ , where  $0 \leq \delta < \alpha_{k-1}$ . Then we have

$$T_{\max} = \sum_{i=1}^{k-2} \alpha_i^2 + (\delta - \alpha_{k-1})^2,$$

and

$$\begin{aligned} G(\mathbf{1}_{\mathcal{S}}) &> -T_{\max} + \sum_{i=1}^{k-2} \alpha_i^2 = \alpha_{k-1}^2 - (\delta - \alpha_{k-1})^2 + \sum_{i=k}^{K^2} \alpha_i^2 \\ &= \delta(2\alpha_{k-1} - \delta) + \sum_{i=k}^{K^2} \alpha_i^2 \geq \alpha_{k-1} \delta + \sum_{i=k}^{K^2} \alpha_i^2 = \frac{M}{2}. \end{aligned}$$

Therefore,

$$\frac{G(\mathbf{1}_{\mathcal{S}})}{G(\mathbf{x}^*)} > \frac{\frac{M}{2}}{-\frac{1}{4} \frac{M^2}{\sum_{i=1}^K \sum_{j=1}^K \alpha_{ij}^2} + M} = \frac{2}{4 - \frac{M}{\sum_{i=1}^K \sum_{j=1}^K \alpha_{ij}^2}}.$$

Note that  $\frac{M}{\sum_{i=1}^K \sum_{j=1}^K \alpha_{ij}^2} = \frac{\max_{\mathbf{x} \in \mathcal{H}} D^T \mathbf{x}}{\frac{1}{2} D^T \mathbf{1}_N} \geq \frac{2(N-L)}{N}$ , then we get the result.

In this proof, we give an upper bound of  $G(\mathbf{1}_{\mathcal{S}^*})$  and a lower bound of  $G(\mathbf{1}_{\mathcal{S}})$  respectively. Based on this, the approximation factor of FFW is given. ■

Note that the approximation factors of continuous greedy algorithm and FrameSense with regard to  $G(\mathbf{x})$  are both  $1 - \frac{1}{e}$ . Thus, if  $L < \frac{N}{e-1}$ , the approximation factor of FFW given by Theorem 2 is better than continuous greedy algorithm and FrameSense.

According to the proof of Theorem 2 in [11], we directly derive a bound with regard to the frame potential from Theorem 2.

*Theorem 3:* Suppose that  $\Psi \in \mathbb{R}^{N \times K}$  satisfies the condition of Theorem 2. Denote by  $\mathcal{S}^*$  an optimal solution of Problem (5) with  $R = 1$ . The set  $\mathcal{S}$  obtained from Algorithm 1 is near optimal with respect to FP as  $F(\mathcal{S}) \leq \gamma F(\mathcal{S}^*)$  with  $\gamma = \frac{1}{N+L} \left( F(\emptyset) \frac{KL}{L_{\min}^2} + N \right)$ , and  $L_{\min} = \min_{|\mathcal{C}|=L} \sum_{i \in \mathcal{C}} \|u_i\|_2^2$ , being  $u_i$  the  $i$ -th row of  $\Psi$ .

## V. ALGORITHM TO SAMPLING TENSORS

In this section, we focus on the most general situation of Problem (5) with  $R \geq 2$ . For convenience, let  $p_{ab}^r$  be the  $(a, b)$ -element of  $\Psi_r$  and  $P_i^r$  be the  $i$ -th column of  $\Psi_r$ ,  $r = 1, \dots, R$ .

### A. The Algorithm

#### Algorithm 2 Fast Frank-Wolfe Algorithm for Tensor Signals

**Input:**  $\Psi_r = (p_{ab}^r) \in \mathbb{R}^{N_r \times K_r}$ ,  $r = 1, \dots, R$ ;  $L$

1: **For**  $r = 1 \dots R$  **do**

2:   Compute  $m_{ij}^r = P_i^{rT} P_j^r$ ,  $i, j = 1, \dots, K_r$

3:   Compute  $F^r = \sum_{i=1}^{K_r} \sum_{j=1}^{K_r} (m_{ij}^r)^2$

4:   Compute  $d_n^r = \frac{1}{F^r} \sum_{i=1}^{K_r} \sum_{j=1}^{K_r} m_{ij}^r p_{ni}^r p_{nj}^r$ ,  
 $n = 1, \dots, N_r$ , and denote  $\mathcal{D}_r = \{d_1^r, d_2^r, \dots, d_{N_r}^r\}$

5: **End**

6: Select the  $N - L$  elements with the biggest values  $\bigcup_{r=1}^R \{d_{l_1^r}^r, \dots, d_{l_{N-L}^r}^r\}$  from  $\bigcup_{r=1}^R \mathcal{D}_r$  such that  $\sum_{r=1}^R S_r = N - L$  and  $S_r \leq N_r - K_r$ ,  $r = 1, \dots, R$

7: **Return:**  $\mathcal{S} = \bigcup_{r=1}^R \{l_1^r, \dots, l_{S_r}^r\}$

The computational complexity of step 1 to step 5 is  $\mathcal{O}(N_{\max} K_{\max}^2)$  with  $N_{\max} = \max_r N_r$  and  $K_{\max} = \max_r K_r$ . The computational complexity of step 6 is  $\mathcal{O}(N)$ . Therefore, the total computational complexity of Algorithm 2 is  $\mathcal{O}(N_{\max} K_{\max}^2)$ , which is much lower than Greedy FP ( $\mathcal{O}(N_{\max}^2 K_{\max}^2)$ ) and UB-FMBS ( $\mathcal{O}(\prod_{r=1}^R N_r)$ ) proposed in [12] and [15], respectively.

### B. Near-optimality of FFW for Tensor Signals

In order to represent  $\tilde{F}(\mathbf{x})$  as the sum of  $R$  terms, we denote

$$\begin{aligned} W(\mathbf{x}) &= \log \left\{ \tilde{F}(\mathbf{0}) \right\} - \log \left\{ \tilde{F}(\mathbf{x}) \right\} \\ &= \sum_{r=1}^R \log \left\{ \tilde{F}_r(\mathbf{0}) \right\} - \sum_{r=1}^R \log \left\{ \tilde{F}_r(\mathbf{x}^r) \right\} \\ &= \sum_{r=1}^R \log \left\{ \sum_{i=1}^{K_r} \sum_{j=1}^{K_r} \left[ \sum_{n=1}^{N_r} p_{ni}^r p_{nj}^r \right]^2 \right\} \\ &\quad - \sum_{r=1}^R \log \left\{ \sum_{i=1}^{K_r} \sum_{j=1}^{K_r} \left[ \sum_{n=1}^{N_r} (1 - x_n^r) p_{ni}^r p_{nj}^r \right]^2 \right\}. \end{aligned}$$

Then we introduce the following problem as surrogate for Problem (5),

$$\begin{aligned} &\max_{\mathbf{x}} W(\mathbf{x}) \\ \text{s.t.} \quad &\|\mathbf{x}\|_1 = N - L \\ &x_i^r = 0 \text{ or } 1, \quad i = 1, \dots, N_r, \quad r = 1, \dots, R. \end{aligned} \quad (9)$$

Now, we can derive the approximation factor of Algorithm 2 by Problem (9).

*Theorem 4:* Denote by  $\mathcal{S}^*$  an optimal solution of Problem (5). If  $P_i^{rT} P_j^r > 0$  and  $p_{ni}^r p_{nj}^r \geq 0$ ,  $n = 1, \dots, N$  for any  $i, j = 1, \dots, K_r$  and  $r = 1, \dots, R$ , then the set  $\mathcal{S} = \bigcup_{r=1}^R \mathcal{S}_r$  obtained from Algorithm 2 is near optimal with respect to FP as  $F(\mathcal{S}) < e^{M - \frac{M^2}{2R} + o(\|\mathbf{1}_{\mathcal{S}}\|^3)} - o(\|\mathbf{1}_{\mathcal{S}^*}\|^3)} F(\mathcal{S}^*)$  with

$$M = \sum_{r=1}^R \frac{2}{F_r(\emptyset)} \sum_{i=1}^{K_r} \sum_{j=1}^{K_r} (P_i^{rT} P_j^r) \sum_{t \in \mathcal{S}_r} p_{ti}^r p_{tj}^r \in (0, 2R).$$

*Proof:* Let  $\mathcal{H}_r = \{\mathbf{x}^r \in \{0, 1\}^{N_r} \mid \|\mathbf{x}^r\|_1 \leq N_r - K_r\}$ ,  $r = 1, \dots, R$  and  $\mathcal{H} = \{(\mathbf{x}^1, \mathbf{x}^2, \dots, \mathbf{x}^R) \in \mathbb{R}^N \mid \mathbf{x}^r \in \mathcal{H}_r, \|\mathbf{x}\|_1 = N - L, r = 1, \dots, R\}$ . For convenience, we denote

$$D_t^r = \left. \frac{\partial \tilde{F}_r(\mathbf{x}^r)}{\partial x_t^r} \right|_{\mathbf{x}=\mathbf{0}} = -2 \sum_{i=1}^{K_r} \sum_{j=1}^{K_r} (P_i^{rT} P_j^r) p_{ti}^r p_{tj}^r,$$

$$F^r = \tilde{F}_r(\mathbf{0}) = \sum_{i=1}^{K_r} \sum_{j=1}^{K_r} (P_i^{rT} P_j^r)^2$$

and

$$B_{st}^r = \frac{\partial^2 \tilde{F}_r(\mathbf{x}^r)}{\partial x_t^r \partial x_s^r} = 2 \sum_{i=1}^{K_r} \sum_{j=1}^{K_r} (p_{ti}^r p_{tj}^r) (p_{si}^r p_{sj}^r).$$

Thus,

$$\left. \frac{\partial W(\mathbf{x})}{\partial x_t^r} \right|_{\mathbf{x}=\mathbf{0}} = -\frac{D_t^r}{F^r}, \quad \left. \frac{\partial^2 W(\mathbf{x})}{\partial x_t^r \partial x_s^r} \right|_{\mathbf{x}=\mathbf{0}} = -\frac{B_{st}^r \cdot F^r - D_s^r D_t^r}{(F^r)^2}.$$

One can see that  $\mathbf{1}_{\mathcal{S}} \in \arg \max_{\mathbf{x} \in \mathcal{H}} \sum_{r=1}^R \sum_{i=1}^{N_r} -\frac{D_i^r}{F^r} x_i^r$  as  $\mathcal{S}$  is obtained by Algorithm 2. Using Maclaurin expansion, we get

$$\begin{aligned} W(\mathbf{x}) &= -\sum_{r=1}^R \left\{ \frac{1}{2(F^r)^2} \sum_t \sum_s x_t^r x_s^r (B_{st}^r \cdot F^r - D_s^r D_t^r) \right\} \\ &\quad + \sum_{r=1}^R \left\{ -\frac{1}{F^r} \sum_{t=1}^{N_r} x_t^r D_t^r \right\} + o(\|\mathbf{x}\|^3) \\ &= \sum_{r=1}^R \frac{1}{F^r} \left\{ \left( -\sum_{t=1}^{N_r} x_t^r D_t^r \right) - \frac{1}{2} \sum_t \sum_s x_t^r x_s^r B_{st}^r \right\} \\ &\quad + \sum_{r=1}^R \left\{ \frac{1}{2(F^r)^2} \left( -\sum_{t=1}^{N_r} x_t^r D_t^r \right)^2 \right\} + o(\|\mathbf{x}\|^3). \end{aligned}$$

Let  $|\mathcal{S}_r| = S_r$ ,  $|\mathcal{S}_r^*| = S_r^*$  and  $\mathcal{U}_r(I) = \{\mathbf{x}^r \in \{0, 1\}^{N_r} \mid \|\mathbf{x}^r\|_1 = I\}$ ,  $r = 1, \dots, R$ , where  $I$  is an integer. Denote  $M_r = -\sum_{t \in \mathcal{S}_r} D_t^r$ ,  $M_r^* = \max_{\mathbf{x}^r \in \mathcal{U}_r(S_r^*)} -\sum_{t=1}^{N_r} x_t^r D_t^r$  and  $M = \sum_{r=1}^R \frac{M_r}{F^r}$ . Clearly,  $\mathcal{U}_r(S_r), \mathcal{U}_r(S_r^*) \subset \mathcal{H}_r$ , thus  $\sum_{r=1}^R \frac{M_r^*}{F^r} \leq M$  as  $\mathbf{1}_{\mathcal{S}}$  belongs to  $\arg \max_{\mathbf{x} \in \mathcal{H}} \sum_{r=1}^R \sum_{i=1}^{N_r} -\frac{D_i^r}{F^r} x_i^r$ .

Note that  $F^r = -\frac{1}{2} \sum_{i=1}^{N_r} D_i^r$ , we have  $0 \leq M_r(M_r^*) \leq 2F^r$  and  $0 \leq M \leq 2R$ . By the proof of Theorem 2, for  $\mathbf{x} = \mathbf{1}_{S^*}$  and  $r = 1, \dots, R$  we have

$$\begin{aligned} & \left( -\sum_{t=1}^{N_r} x_t^r D_t^r \right) \leq M_r^*, \\ & \left( -\sum_{t=1}^{N_r} x_t^r D_t^r \right) - \frac{1}{2} \sum_t \sum_s x_t^r x_s^r B_{st}^r < M_r^* - \frac{(M_r^*)^2}{4F^r}. \end{aligned}$$

Then we obtain

$$\begin{aligned} W(\mathbf{1}_{S^*}) &< \sum_{r=1}^R \left\{ \frac{1}{2} \left( \frac{M_r^*}{F^r} \right)^2 + \frac{1}{F^r} \left( M_r^* - \frac{(M_r^*)^2}{4F^r} \right) \right\} \\ &+ o(\|\mathbf{1}_{S^*}\|^3) \\ &< \sum_{r=1}^R \left\{ \frac{1}{4} \left( \frac{M_r^*}{F^r} \right)^2 + \frac{M_r^*}{F^r} \right\} + o(\|\mathbf{1}_{S^*}\|^3) \\ &= \frac{1}{4} \sum_{r=1}^R \left( \frac{M_r^*}{F^r} + 2 \right)^2 - R + o(\|\mathbf{1}_{S^*}\|^3). \end{aligned} \quad (10)$$

Denote by  $Q_{max}$  the value of

$$\begin{aligned} & \max_{y_1, y_2, \dots, y_R} \sum_{r=1}^R (y_r + 2)^2 \\ & \text{s.t. } 0 \leq y_r \leq 2 \\ & \sum_{r=1}^R y_r \leq M. \end{aligned}$$

Let  $M = 2m + \delta$ , in which  $m$  is an integer and  $\delta \in [0, 2)$ . One can verify that  $Q_{max} = m(2+2)^2 + (\delta+2)^2 + (R-m-1) \cdot (0+2)^2 = 12m + \delta^2 + 4\delta + 4R$ . Thus,

$$\begin{aligned} W(\mathbf{1}_{S^*}) &< \frac{1}{4} (12m + \delta^2 + 4\delta + 4R) - R + o(\|\mathbf{1}_{S^*}\|^3) \\ &< \frac{1}{4} (12m + 6\delta + 4R) - R + o(\|\mathbf{1}_{S^*}\|^3) \\ &= \frac{3}{2}M + o(\|\mathbf{1}_{S^*}\|^3). \end{aligned} \quad (11)$$

Again by the proof of Theorem 2, for  $\mathbf{x} = \mathbf{1}_S$  and  $r = 1, \dots, R$ , we get

$$\begin{aligned} & \left( -\sum_{t=1}^{N_r} x_t^r D_t^r \right) = M_r, \\ & \left( -\sum_{t=1}^{N_r} x_t^r D_t^r \right) - \frac{1}{2} \sum_t \sum_s x_t^r x_s^r B_{st}^r > \frac{M_r}{2}. \end{aligned}$$

Thus, we obtain

$$\begin{aligned} W(\mathbf{1}_S) &> \sum_{r=1}^R \left\{ \frac{1}{2(F^r)^2} (M_r)^2 + \frac{1}{F^r} \left( \frac{M_r}{2} \right) \right\} \\ &+ o(\|\mathbf{1}_S\|^3) \\ &= \frac{1}{2} \sum_{r=1}^R \left( \frac{M_r}{F^r} + \frac{1}{2} \right)^2 - \frac{R}{8} + o(\|\mathbf{1}_S\|^3). \end{aligned} \quad (12)$$

Denote by  $Q_{min}$  the value of

$$\begin{aligned} & \min_{y_1, y_2, \dots, y_R} \sum_{r=1}^R \left( y_r + \frac{1}{2} \right)^2 \\ & \text{s.t. } 0 \leq y_r \leq 2 \\ & \sum_{r=1}^R y_r \leq M. \end{aligned}$$

Obviously,  $Q_{min} = R \left( \frac{M}{R} + \frac{1}{2} \right)^2$ . Then we have

$$\begin{aligned} W(\mathbf{1}_S) &> \frac{R}{2} \left( \frac{M}{R} + \frac{1}{2} \right)^2 - \frac{R}{8} + o(\|\mathbf{1}_S\|^3) \\ &= \frac{M^2}{2R} + \frac{M}{2} + o(\|\mathbf{1}_S\|^3). \end{aligned}$$

By (11) and (12), we have

$$\begin{aligned} & W(\mathbf{1}_S) - W(\mathbf{1}_{S^*}) \\ &= -\log \left\{ \tilde{F}(\mathbf{1}_S) \right\} + \log \left\{ \tilde{F}(\mathbf{1}_{S^*}) \right\} \\ &= \log \frac{\tilde{F}(\mathbf{1}_{S^*})}{\tilde{F}(\mathbf{1}_S)} \\ &> \frac{M^2}{2R} + \frac{M}{2} - \frac{3}{2}M + o(\|\mathbf{1}_S\|^3) - o(\|\mathbf{1}_{S^*}\|^3) \\ &= \frac{M^2}{2R} - M + o(\|\mathbf{1}_S\|^3) - o(\|\mathbf{1}_{S^*}\|^3), \end{aligned}$$

thus

$$\begin{aligned} & \frac{\tilde{F}(\mathbf{1}_{S^*})}{\tilde{F}(\mathbf{1}_S)} > e^{\frac{M^2}{2R} - M + o(\|\mathbf{1}_S\|^3) - o(\|\mathbf{1}_{S^*}\|^3)} \\ & \Rightarrow \tilde{F}(\mathbf{1}_S) < e^{M - \frac{M^2}{2R} + o(\|\mathbf{1}_S\|^3) - o(\|\mathbf{1}_{S^*}\|^3)} \tilde{F}(\mathbf{1}_{S^*}) \\ & \Rightarrow F(\mathcal{S}) < e^{M - \frac{M^2}{2R} + o(\|\mathbf{1}_S\|^3) - o(\|\mathbf{1}_{S^*}\|^3)} F(\mathcal{S}^*). \end{aligned}$$

Since  $F^r = \tilde{F}_r(0) = F_r(\emptyset)$ , we have  $M = \sum_{r=1}^R \frac{M_r}{F^r} = \sum_{r=1}^R \frac{1}{F_r(\emptyset)} \left\{ -\sum_{t \in S_r} D_t^r \right\}$ .

This completes the proof of Theorem 4.  $\blacksquare$

Different from sampling vector signals, the algorithm of sampling tensor signals and the analysis of theoretical boundaries are more complicated. The approximate factor given by Theorem 3 for sampling vectors is more accurate than the bound given by Theorem 4 for sampling tensor, and does not contain infinitesimal terms.

## VI. NUMERICAL RESULTS

### A. Comparison with traditional sampling methods

FrameSense [11] is a classical method to sampling vectors, which uses greedy algorithm to optimize FP, and also gives the approximate factor. Greedy FP [12] extends FrameSense to sampling tensors. FMBS [15] is the latest algorithm for sampling vectors, and its computational complexity and solution quality are the best so far. In this section, we experimentally compare the performance of FFW with these methods and Random sampling.

For vector signals, we use 100 different instances and compute the average MSE as a function of  $L$ . We randomly generate a matrix  $\Psi \in \mathbb{R}^{200 \times 40}$  for each of these instances.

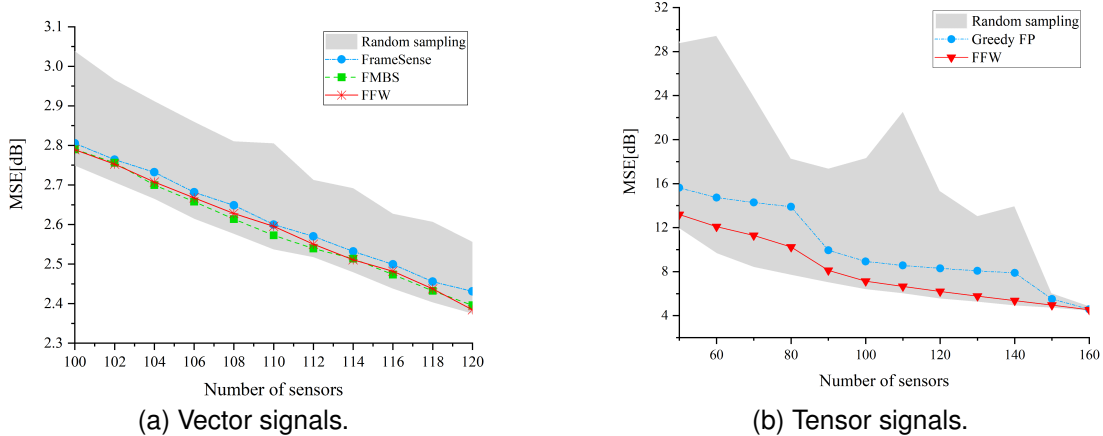


Fig. 1. Comparison in terms of MSE of FFW, FrameSense, FMBS, Greedy FP and random sampling for vector and tensor signals.

Then, we compare the performance of FFW with random sampling, FrameSense and FMBS. Random sampling is based on randomly selecting rows of  $\Psi$  for 500 times. Since the performance is measured in terms of MSE, the lower the curve, the higher the performance. The results are shown in Figure 1a. The shaded area represent the interval of random sampling. Figure 1a shows that FFW performs as well as FMBS, and has a slight advantage over FrameSense.

Then we perform the experiment with 3-order tensor signals. We also use 100 different instances to compare the performance of FFW with random sampling and Greedy FP. In each instance, we randomly generate three matrices  $\{\Psi_i \in \mathbb{R}^{N_i \times K_i}\}_{i=1}^{R=3}$  with  $N_1 = 50, N_2 = 60, N_3 = 70, K_1 = 10, K_2 = 20, K_3 = 15$  and solve Problem (5) for different number of sensors. The results are shown in Figure 1b. It can be seen that FFW performs much better than Greedy FP in terms of MSE. And the larger  $L$  is, the closer the result of FFW is to the optimal results of random sampling.

In the third experiment, for tensor signals, we randomly draw six matrices  $\Psi \in \mathbb{R}^{N \times K}$  with  $K = 40$  and  $N \in \{100, 150, 200, 250, 300, 350, 400\}$ , while we place  $L = 0.5N$  sensors for vector signals. And for tensor signals, we draw matrices  $\{\Psi_i \in \mathbb{R}^{N_i \times K_i}\}_{i=1}^{R=3}$  with dimensions  $K_1 = 10, K_2 = 20$  and  $K_3 = 15$ , while  $(N_1, N_2, N_3) \in \{(30 + \omega, 40 + \omega, 50 + \omega) | \omega = 0, 10, 20, 30, 40, 50, 60\}$ . We measure the computational time together with the MSE, showing that for vector signals, while FFW is significantly faster than FMBS and FrameSense, the difference in MSE is minimal (Figure 2a). Moreover, when sampling tensor signals, the gap of computational time between FFW and Greedy FP is greater, and the MSE performance of FFW is also better than Greedy FP (Figure 2b).

### B. Sampling and reconstruction of image data

In this subsection, we used a classical demo image in MATLAB called “Peppers” for performance comparison. We first used FFW and Greedy FP for sampling real-world image data and use the least squares method to reconstruction. Then, we randomly select  $L$  rows and columns of image data, and

apply Convolutional Conditional Neural Process (ConvCNP) [21] as the model to completion.

In first experiment, we performed singular value decomposition on this image  $\mathbf{X} = \mathbf{U}_1 \Sigma \mathbf{U}_2^\top$  and then used the first  $K_1$  columns of  $\mathbf{U}_1$  and  $K_2$  column of  $\mathbf{U}_2$  as two factor matrices for sampling and reconstruction. We set the dimension of low-dimensional parameter matrix to be  $40 \times 40$ , i.e.,  $K_1 = 40$  and  $K_2 = 40$ . Let the number of sensors  $L = 400$ . The results are showed in Figure 3. One can see that MSE of sampling by Greedy FP is much bigger than MSE of sampling by FFW.

Then, we randomly sample the image data, and complete it by ConvCNP. The number of sensors  $L$  is 400, 600, 700 and 800 respectively.

ConvCNP combines a convolutional neural network with features of a Gaussian process to model the conditional distribution of inputs as a way of dealing with uncertainty modeling between input-output pairs. Compared to traditional point-based prediction models, ConvCNP is able to make high-quality predictions on unobserved data by modeling conditional distributions with a small amount of observed data. ConvCNP is suitable for a range of canonical machine learning tasks, including regression, classification and image completion [21].

We choose the CIFAR10 [22] dataset, a commonly used dataset for image completion task. The CIFAR10 dataset is of moderate size, containing 10 categories of color images with 6000  $32 \times 32$  RGB images in each category. These categories cover different items and scenes in daily life, which can enable the generative model to learn the features among different categories and generate images with generalization. Using the public data set CIFAR10, we train the ConvCNP model for 200 epochs using Adam [23] with learning rate of  $5 \times 10^{-4}$ , batch size of 256. We input the original image “Peppers” and control the proportion of the original image to be masked by setting the masking factor. Since the model needs to complement the images masked by random whole rows and columns in the testing phase, we train the model by randomly selecting whole rows and columns to mask images. After the training is completed, we save the optimal model parameters. Then we convert the masked matrix into a grayscale image to match

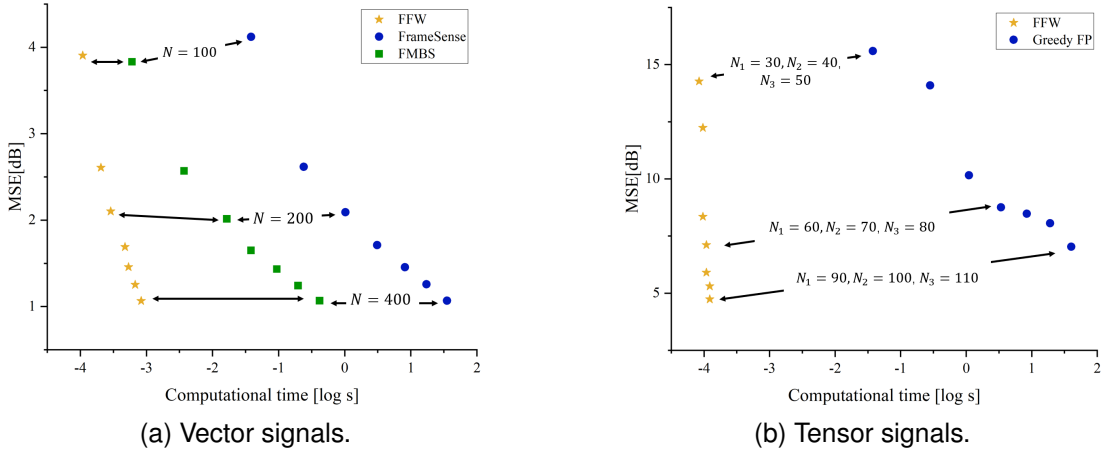


Fig. 2. Analysis of the tradeoff between computational time and MSE for FFW with FMBS, FrameSense and Greedy FP

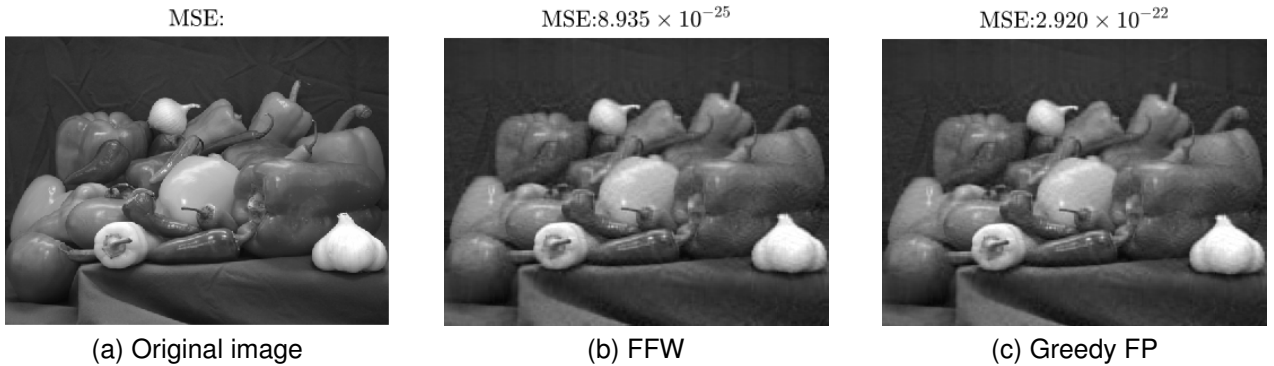


Fig. 3. Visualization of different sampling and reconstruction results of real-world image (“Peppers”).

the number of channels (the number of channels in CIFAR10 dataset is 3), and then input the image into the model as an observation for image completion. The results can be seen in Figure 4.

Obviously, the results completed by convCNP is not as good as those reconstructed by least squares method (Figure 3). Usually, the predictive performance of an intelligent model is highly dependent on the number of context points [24]–[26]. Although the ConvCNP model can predict masked regions well given a few context points, the fewer the context points, the greater the uncertainty of the model prediction. In the experiments, the model omits a lot of contextual information by masking images with whole rows and columns, resulting in reducing the prediction accuracy of the model. In addition, intelligent models require high computational resources and high time costs. However, under the model of this paper, using the singular value decomposition of the image data, the core is reconstructed by the least square method after fast sampling, so that the original image can be reconstructed more quickly and accurately.

## VII. CONCLUSION

In this paper, we proposed a fast algorithm (FFW) to sampling for inverse problems with vectors and tensors. We first provide closed-form multilinear extensions for the frame

potential of pruned matrices (Theorem 1). For faster sampling, we design FFW to sampling vectors with complexity  $\mathcal{O}(NK^2)$ , and extend FFW to sampling high-order tensors with complexity  $\mathcal{O}(N_{\max}K_{\max}^2)$ . We also give the approximation factor of FFW for a special class of sampling matrices (Theorem 3 and 4). Then, we experimentally demonstrate the strength of FFW in performance and running time, compared with FrameSense, FMBS and Greedy FP. Finally, we show that for image data, the results of using FFW sampling and least squares reconstruction are better than the results of using convCNP completion after random sampling.

## REFERENCES

- [1] A. Cichocki, D. Mandic, L. De Lathauwer, G. Zhou, Q. Zhao, C. Caiafa, and H. A. PHAN, “Tensor decompositions for signal processing applications: From two-way to multiway component analysis,” *IEEE Signal Processing Magazine*, vol. 32, no. 2, pp. 145–163, 2015.
- [2] N. D. Sidiropoulos, L. De Lathauwer, X. Fu, K. Huang, E. E. Papalexakis, and C. Faloutsos, “Tensor decomposition for signal processing and machine learning,” *IEEE Transactions on Signal Processing*, vol. 65, no. 13, pp. 3551–3582, 2017.
- [3] C. Groetsch, “Linear inverse problems,” in *Handbook of mathematical methods in imaging*, 2015.
- [4] F. Wang, Y. Wang, G. Cheung, and C. Yang, “Graph sampling for matrix completion using recurrent gershgorin disc shift,” *IEEE Transactions on Signal Processing*, vol. 68, pp. 2814–2829, 2020.
- [5] H. Jamali-Rad, A. Simonetto, X. Ma, and G. Leus, “Distributed sparsity-aware sensor selection,” *IEEE Transactions on Signal Processing*, vol. 63, no. 22, pp. 5951–5964, 2015.



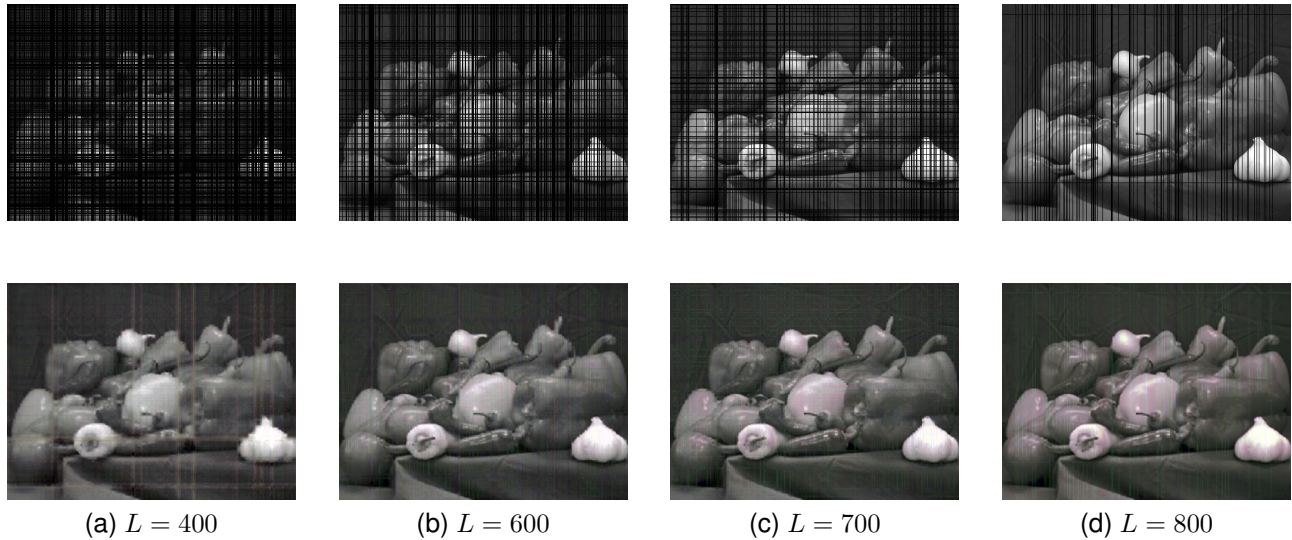


Fig. 4. Visualization of using convCNP completion after random sampling of real-world image (“Peppers”).

- [6] P. Ghamisi, N. Yokoya, J. Li, W. Liao, S. Liu, J. Plaza, B. Rasti, and A. Plaza, “Advances in hyperspectral image and signal processing: A comprehensive overview of the state of the art,” *IEEE Geoscience and Remote Sensing Magazine*, vol. 5, no. 4, pp. 37–78, 2017.
- [7] G. Liu, Q. Liu, and X. Yuan, “A new theory for matrix completion,” in *Advances in Neural Information Processing Systems*, I. Guyon, U. V. Luxburg, S. Bengio, H. Wallach, R. Fergus, S. Vishwanathan, and R. Garnett, Eds., vol. 30. Curran Associates, Inc., 2017, p. 785–794.
- [8] C. Jiang, Y. C. Soh, and H. Li, “Sensor placement by maximal projection on minimum eigenspace for linear inverse problems,” *IEEE Transactions on Signal Processing*, vol. 64, no. 21, pp. 5595–5610, 2016.
- [9] S. Joshi and S. Boyd, “Sensor selection via convex optimization,” *IEEE Transactions on Signal Processing*, vol. 57, no. 2, pp. 451–462, 2009.
- [10] C. Jiang, Z. Chen, R. Su, and Y. C. Soh, “Group greedy method for sensor placement,” *IEEE Transactions on Signal Processing*, vol. 67, no. 9, pp. 2249–2262, 2019.
- [11] J. Ranieri, A. Chebira, and M. Vetterli, “Near-optimal sensor placement for linear inverse problems,” *IEEE Transactions on Signal Processing*, vol. 62, no. 5, pp. 1135–1146, 2014.
- [12] G. Ortiz-Jiménez, M. Coutino, S. P. Chepuri, and G. Leus, “Sparse sampling for inverse problems with tensors,” *CoRR*, vol. abs/1806.10976, 2018.
- [13] C. I. Kanatsoulis, X. Fu, N. D. Sidiropoulos, and M. Akçakaya, “Tensor completion from regular sub-nyquist samples,” *IEEE Transactions on Signal Processing*, vol. 68, pp. 1–16, 2020.
- [14] C. I. Kanatsoulis and N. D. Sidiropoulos, “Large-scale canonical polyadic decomposition via regular tensor sampling,” in *2019 27th European Signal Processing Conference (EUSIPCO)*, 2019, pp. 1–5.
- [15] F. Wang, G. Cheung, T. Li, Y. Du, and Y.-P. Ruan, “Fast sampling and reconstruction for linear inverse problems: From vectors to tensors,” *IEEE Transactions on Signal Processing*, vol. 70, pp. 6376–6391, 2022.
- [16] S. Liu and O. Trenkler, “Hadamard, khatri-rao, kronecker and other matrix products,” *int.j.inf.syst.sci*, 2008.
- [17] A. Cichocki, D. Mandic, L. De Lathauwer, G. Zhou, Q. Zhao, C. Caiafa, and H. A. PHAN, “Tensor decompositions for signal processing applications: From two-way to multiway component analysis,” *IEEE Signal Processing Magazine*, vol. 32, no. 2, pp. 145–163, 2015.
- [18] M. Fickus, D. G. Mixon, and M. J. Poteet, “Frame completions for optimally robust reconstruction,” *Wavelets and Sparsity XIV*, 2011.
- [19] J. Vondrak, “Optimal approximation for the submodular welfare problem in the value oracle model,” in *Proceedings of the Fortieth Annual ACM Symposium on Theory of Computing*, ser. STOC ’08. New York, NY, USA: Association for Computing Machinery, 2008, p. 67–74.
- [20] M. Frank and P. Wolfe, “An algorithm for quadratic programming,” *Naval Research Logistics Quarterly*, vol. 3, no. 1-2, pp. 95–110, 1956.
- [21] J. Gordon, W. P. Bruinsma, A. Y. Foong, J. Requeima, Y. Dubois, and R. E. Turner, “Convolutional conditional neural processes,” *arXiv preprint arXiv:1910.13556*, 2019.
- [22] A. Krizhevsky and G. Hinton, “Learning multiple layers of features from tiny images,” *Handbook of Systemic Autoimmune Diseases*, vol. 1, no. 4, 2009.
- [23] D. P. Kingma and J. Ba, “Adam: A method for stochastic optimization,” *arXiv preprint arXiv:1412.6980*, 2014.
- [24] M. Garnelo, J. Schwarz, D. Rosenbaum, F. Viola, D. J. Rezende, S. Eslami, and Y. W. Teh, “Neural processes,” *arXiv preprint arXiv:1807.01622*, 2018.
- [25] H. Kim, A. Mnih, J. Schwarz, M. Garnelo, A. Eslami, D. Rosenbaum, O. Vinyals, and Y. W. Teh, “Attentive neural processes,” *arXiv preprint arXiv:1901.05761*, 2019.
- [26] M. Garnelo, D. Rosenbaum, C. Maddison, T. Ramalho, D. Saxton, M. Shanahan, Y. W. Teh, D. Rezende, and S. A. Eslami, “Conditional neural processes,” in *International conference on machine learning*. PMLR, 2018, pp. 1704–1713.